



Methyl transfer reactivity of pentachloromethylplatinate(IV) anion with a series of *N*-nucleophiles

Daniel J. Adams, Brian Johns, Andrei N. Vedernikov*

Department of Chemistry and Biochemistry, University of Maryland, College Park, MD, 20742, USA

ARTICLE INFO

Article history:

Received 4 October 2018

Received in revised form

22 October 2018

Accepted 23 October 2018

Available online 26 October 2018

This work is dedicated to Prof. Richard J. Puddephatt on the occasion of his 75th birthday.

Keywords:

Pentachloromethylplatinate(IV)

Anilines

Pyridines

Methyl transfer

Kinetics

Aqueous acetone

ABSTRACT

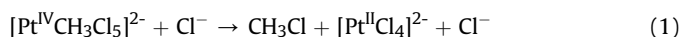
Reactivity of $K_2[Pt^{IV}CH_3Cl_5]$ toward a series of substituted *N,N*-dimethylanilines **1a–1g**, *N,N*-diisopropylaniline **1h** and 2,6-substituted pyridines **2a–2b** was investigated in 60% (vol.) aqueous acetone solutions. The reactions result in corresponding *N*-methylammonium or *N*-methylpyridinium products, **3** or **4**, with high selectivity for the substrates **1a–1g** and **2b**, and follow an overall 2nd order kinetics, 1st order in both the Pt^{IV} complex and the amines. The reactivity is discussed in terms of the amine electronic properties and steric bulk. For the series of *N,N*-dimethylanilines **1a–1g**, $Me_2NC_6H_4R$ ($R = H, m\text{-Cl}, p\text{-Cl}, m\text{-Me}, p\text{-Me}, p\text{-MeO}, p\text{-Me}_2N$), a high quality linear correlation was found between logarithm of the reaction second order rate constant, $\log(k_2)$, and pK_a of the anilines. At the same time, the reactivity of the bulkier *N,N*-diisopropylaniline substrate **1h** is about 3 orders of magnitude lower than predicted using this correlation. Finally, the pyridines **2a–2b** are 3–4 orders of magnitude less reactive than *N,N*-dimethylanilines of similar pK_a . Interestingly, the reactivity of $K_2[Pt^{IV}CH_3Cl_5]$ toward *N,N*-dimethylanilines is of the same order of magnitude or slightly greater than that of a standard organic methylating agent, dimethylsulfate Me_2SO_4 . A computational (DFT) modeling of the title reaction is consistent with the formation of five-coordinate $Pt^{IV}Me$ electrophile, $[Pt^{IV}CH_3Cl_4]^-$, which is involved in S_N2 attack at its methyl group carbon by nucleophilic amines.

© 2018 Elsevier B.V. All rights reserved.

1. Introduction

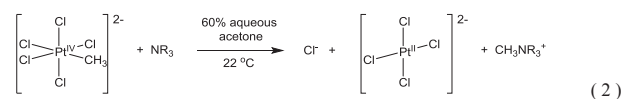
Chloro complexes of platinum(II), such as $Pt^{II}Cl_2(H_2O)_2$, were the first homogeneous transition metal complexes used for catalytic oxidative CH functionalization of methane to form CH_3X derivatives (Scheme 1, $X = Cl, OH$) [1,2]. These complexes are especially attractive as catalysts because they allow for alkane functionalization under aerobic conditions and for the use of O_2 as terminal oxidant when combined with specific redox-mediators [3–5].

The mechanism of the Shilov reaction was studied in detail and the intermediacy of Pt^{IV} chloro methyl complexes such as $[Pt^{IV}CH_3Cl_5]^{2-}$ was demonstrated [2,6]. The relatively stable potassium pentachloromethylplatinate(IV) was used to conduct kinetics studies of bimolecular nucleophilic substitution at the methyl ligand of $[Pt^{IV}CH_3Cl_5]^{2-}$ with chloride (eq 1), water, as well as some other nucleophiles [6].



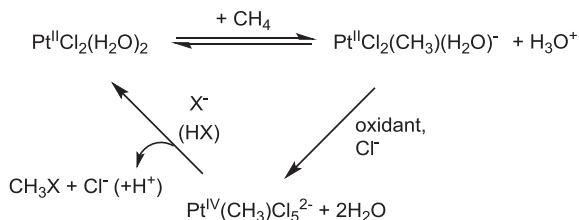
Similar studies were carried out using an analogous Pt^{IV} 2-chloroethyl complex [7]. While important for drawing conclusions about plausible mechanism of the Shilov reaction, these works also open up a horizon for possible application of alkyl transfer from the electrophilic $[Pt^{IV}(Alkyl)Cl_5]^{2-}$ to other nucleophilic species and, potentially, catalytic formation of methane derivatives CH_3X , different from alcohols or alkylchlorides, in modified Shilov systems. To be successful with the latter goal, one needs to know how reactive nucleophiles of other types can be with respect to $[Pt^{IV}(Alkyl)Cl_5]^{2-}$. Notably, amines have never been studied in methyl transfer reactions with $[Pt^{IV}CH_3Cl_5]^{2-}$.

With this idea in mind, in this work we have carried out a kinetics study of methyl transfer from pentachloromethylplatinate(IV) to a series of *N*-nucleophiles, substituted *N,N*-dialkylanilines **1** and pyridines **2** (Chart 1) in 60% (vol.) aqueous acetone solutions at 22 °C (eq 2):



* Corresponding author.

E-mail address: avederni@umd.edu (A.N. Vedernikov).



Scheme 1. Methane CH functionalization catalyzed by $\text{Pt}^{\text{II}}(\text{Cl}_2)(\text{H}_2\text{O})_2$ in the Shilov system.

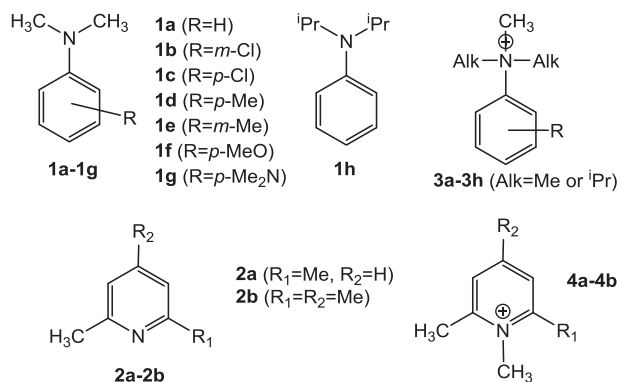


Chart 1. Amine nucleophiles **1** and **2** studied in this work and products of their N -methylation, **3** and **4** (eq 2).

The reaction (eq 2) progress was monitored by means of ^1H NMR spectroscopy. Triflate salts derived from N,N,N -trimethylanilinium cations **3a–3h** and N -methylpyridinium cations **4a–4b**, have been prepared independently and their ^1H NMR spectra were matched to the NMR spectra of the reaction (eq 2) products.

Recently Goldberg et al. reported methyl transfer reactions involving a Rh^{III} diiodo methyl complex $(\text{POP})\text{Rh}^{\text{III}}(\text{CH}_3)_2$ and various alkylamines [8], where formation of an electrophilic cationic $(\text{POP})\text{Rh}^{\text{III}}(\text{CH}_3)(\text{amine})^+$ species occurs first as a result of an amine for iodo ligand substitution. The resulting cationic species are sufficiently electrophilic to be attacked, at the rate determining step, by second equivalent of the amine to form products of the amine methylation. Overall, the methyl transfer reaction between $(\text{POP})\text{Rh}^{\text{III}}(\text{CH}_3)_2$ and alkylamines is second order in alkylamines.

In contrast to the above report, in this work we find that the reaction (eq 2) rate is 1st order in both the amine and $[\text{Pt}^{\text{IV}}\text{CH}_3\text{Cl}_5]^{2-}$, and the reaction is, overall, 2nd order. We also find that for all N,N -dimethylanilines **1a–1g** studied here, there is a high quality linear correlation between logarithm of their second order rate constant, $\log(k_2)$, and the amines $\text{p}K_{\text{a}}$ values. A significant deviation from this dependence is only found here for N,N -diisopropylaniline **1h** and it is discussed in terms of the amine steric bulk.

2. Experimental details

2.1. General procedures

All reagents for which the synthesis is not given were purchased from Aldrich, Acros or Alfa-Aesar and were used without further purification except where stated. Deuterated solvents were purchased from Cambridge Isotope Laboratories (D_2O , acetone- d_6 and $\text{DMSO}-d_6$). ^1H (600 MHz) and ^{13}C NMR (125 MHz) spectra were recorded on a Bruker DRX-500 or Bruker AVIII-600MHz

spectrometer. Chemical shifts are reported in parts per million (ppm) (δ) and referenced to residual solvent resonance peaks. Mixed solvent samples are referenced to acetone- d_6 residual signal. Multiplicities are reported as follows: s (singlet), d (doublet), t (triplet), q (quartet), quin (quintet), sept (septet), m (multiplet). $\text{K}_2[\text{Pt}^{\text{IV}}\text{CH}_3\text{Cl}_5]$ containing KCl as a major impurity was prepared according to published procedure [6]. Anilines **1a**, **1b**, **1d**, **1f**, **1g** and **1h** along with pyridines **2a**, **2b** were purchased from Sigma Aldrich. Anilines **1c** and **1e** were synthesized in accordance with the published procedures [9,10]. Methylammonium salts **3a–g** and **4a**, **4b** were synthesized as triflates according to published procedures [11–17].

2.2. Synthetic procedures

2.2.1. Preparation of $\text{K}_2[\text{PtCl}_5\text{CH}_3]$ [6]

K_2PtCl_4 (426 mg, 1.02 mmol) was dissolved in water and MeI (64.0 μL , 1.02 mmol) was added via microliter syringe. The solution was stirred at rt for 2 h until PtI_2 stopped precipitating. AgCl (152 mg, 1.06 mmol) was added and the mixture was stirred for 20 min. The mixture was filtered and water removed at reduced pressure to give the $\text{K}_2\text{PtCl}_5\text{CH}_3$ product in 73% crude yield. The KCl impurity could not be removed; however this did not affect the kinetics experiments. The KCl-contaminated product contained, typically, ~46% $\text{K}_2\text{PtCl}_5\text{CH}_3$ by mass (about 7: 1 KCl: $\text{K}_2\text{PtCl}_5\text{CH}_3$ molar ratio), as confirmed by ^1H NMR using 1,4-dioxane as an internal standard. ^1H NMR (600 Hz, 22 $^\circ\text{C}$, 60% acetone- d_6 in D_2O) δ : 2.95 (s, 3H); $^2J_{\text{PtH}} = 77$ Hz).

2.2.2. Preparation of anilines **1**

2.2.2.1. 4-Chloro- N,N -dimethylaniline **1c** [9]. ^1H NMR (60% acetone- d_6 in D_2O): δ 7.06 (d, 2H), 6.63 (d, 2H), 2.93 (s, 6H).

2.2.2.2. 3, N,N -trimethylaniline **1e** [10]. ^1H NMR (60% acetone- d_6 in D_2O): δ 7.17 (m, 1H), 6.60 (m, 3H), 2.97 (s, 6H), 2.36 (s, 3H).

2.2.3. Preparation of ammonium triflates **3(OTf)** and **4(OTf)**

2.2.3.1. N,N,N -Trimethylanilinium triflate **3a(OTf)** [11]. ^1H NMR (600 Hz, 22 $^\circ\text{C}$, 60% acetone- d_6 in D_2O) δ : 7.88 (d, 2H), 7.59 (t, 2H), 7.52 (t, 1H), 3.68 (s, 9H).

2.2.3.2. 3-Chloro- N,N,N -trimethylanilinium triflate **3b(OTf)** [12]. ^1H NMR (600 Hz, 22 $^\circ\text{C}$, 60% acetone- d_6 in D_2O) δ : 8.05 (s, 1H), 7.99 (d, 1H), 7.66 (t, 1H), 7.57 (d, 1H), 3.78 (s, 9H).

2.2.3.3. 4-Chloro- N,N,N -trimethylanilinium triflate **3c(OTf)** [13]. ^1H NMR (600 Hz, 22 $^\circ\text{C}$, 60% acetone- d_6 in D_2O) δ : 8.00 (d, 2H), 7.61 (d, 2H), 3.74 (s, 9H).

2.2.3.4. 4, N,N,N -Tetramethylanilinium triflate **3d(OTf)** [14]. ^1H NMR (600 Hz, 22 $^\circ\text{C}$, 60% acetone- d_6 in D_2O) δ : 7.75 (d, 2H), 7.38 (d, 2H), 3.64 (s, 9H), 3.02 (s, 3H).

2.2.3.5. 3, N,N,N -Tetramethylanilinium triflate **3e(OTf)** [15]. ^1H NMR (600 Hz, 22 $^\circ\text{C}$, 60% acetone- d_6 in D_2O) δ : 7.71 (s, 1H), 7.65 (d, 1H), 7.45 (t, 1H), 7.32 (d, 1H), 3.64 (s, 9H), 2.35 (s, 3H).

2.2.3.6. 4-Methoxy- N,N,N -trimethylanilinium triflate **3f(OTf)** [16]. ^1H NMR (600 Hz, 22 $^\circ\text{C}$, 60% acetone- d_6 in D_2O) δ : 7.82 (d, 2H), 7.07 (d, 2H), 3.77 (s, 3H), 3.63 (s, 9H).

2.2.3.7. 4-Dimethylamino- N,N,N -trimethylanilinium **3g(OTf)** [15]. ^1H NMR (600 Hz, 22 $^\circ\text{C}$, 60% acetone- d_6 in D_2O) δ : 7.63 (d, 2H), 6.77 (d, 2H), 3.56 (s, 9H), 2.88 (s, 6H).

2.2.3.8. *N,N*-diisopropyl-*N*-methylanilinium triflate **3h(OTf)**. ^1H NMR (600 Hz, 22 °C, 60% acetone- d_6 in D_2O) δ : 7.71 (d, 2H), 7.59 (t, 2H), 7.54 (t, 1H), 4.54 (sept, 2H), 3.40 (s, 3H), 1.24 (dd, 12H). ^1H NMR (600 Hz, 22 °C, $\text{DMSO}-d_6$) δ : 7.80 (d, 2H), 7.63 (t, 2H), 7.59 (t, 1H), 4.53 (sept, 2H), 3.39 (s, 3H), 1.18 (dd, 12H). ^{13}C NMR (125 Hz, 22 °C, $\text{DMSO}-d_6$) δ : 139.5, 130.5, 130.1, 123.8, 65.8, 40.9, 17.4, 17.1.

2.2.3.9. 1,2,6-Trimethylpyridinium triflate **4a(OTf)** [17]. ^1H NMR (600 Hz, 22 °C, 60% acetone- d_6 in D_2O) δ : 8.18 (t, 1H), 7.74 (d, 2H), 4.08 (s, 3H), 2.77 (s, 6H).

2.2.3.10. 1,2,4,6-Tetramethylpyridinium triflate **4b(OTf)** [17]. ^1H NMR (600 Hz, 22 °C, 60% acetone- d_6 in D_2O) δ : 7.56 (s, 2H), 4.01 (s, 3H), 2.72 (s, 6H), 2.45 (s, 3H).

2.3. Kinetics study

A stock solution of each nucleophile was prepared by adding 1.5 mL of 60% (vol.) acetone- d_6 in D_2O to the appropriate amount of nucleophile via micro syringe. 600 μL of the stock solution was combined with ~2 mg of solid K_2PtCl_5 and quickly transferred to a 5 mm NMR tube and placed into an NMR probe. The reaction progress was followed by ^1H NMR. The peak at 2.95 ppm which corresponds to the methyl group of $\text{K}_2\text{PtCl}_5\text{CH}_3$ and the peak corresponding to the signal of the methyl group of ammonium product were integrated and the values obtained were used to generate pseudo first order kinetics plots for each nucleophile.

Each run was performed under pseudo first order conditions. To find the pseudo-first order rate constant, k_{obs} , for each run, β from equation (3) was plotted against time, where $[\text{Me(amine)}^+\infty]$ represents the concentration of the methylammonium species at the end of the reaction ($t = \text{infinity}$). To get an accurate value for $[\text{Me(amine)}^+\infty]$ at $t = \text{infinity}$, the mixtures were left for 72 h and a final data point was taken for each. The second order rate constant k_2 was produced using equation (4).

$$\beta = \ln \left(\frac{[\text{NMe(amine)}^+\infty]}{[\text{Me(amine)}^+\infty] - [\text{Me(amine)}^+]_t} \right) \quad (3)$$

$$k_2 = k_{\text{obs}}/[\text{amine}] \quad (4)$$

2.4. Computational study

Theoretical calculations in this work have been performed using density functional theory (DFT) method [18], specifically functional PBE [19], and LACVP relativistic basis set with two polarization functions, as implemented in the Jaguar program package [20]. Full geometry optimization has been performed without constraints on symmetry in gas phase. For all transition states solvation Gibbs energies G_{solv} in water as solvent were found using single point calculations utilizing Poisson-Boltzmann continuum solvation model (PBF) [20]. For water as a solute G_{solv} was found using saturated vapor pressure of water at 25 °C [21]. Geometry optimization for $\text{Pt}^{\text{IV}}\text{CH}_3$ species, $\text{K}_2\text{PtCl}_5\text{CH}_3$, **5** and **6**, in water have also been carried out in water as solvent. For all species under investigation frequency analysis has been carried out. All energy minima have been checked for the absence of imaginary frequencies. All transition states possessed just one imaginary frequency. Using method of Intrinsic Reaction Coordinate, reactants, products and the corresponding transition states were proven to be connected by

a single minimal energy reaction path. For gas-phase geometry-optimized species the total gas phase Gibbs free energy (G_{tot}) at 298 K were produced in Hartrees (1 Hartree = 627.51 kcal/mol). The standard reaction Gibbs energies, ΔG_{rxn} , in kcal/mol were calculated as follows:

$$\Delta G_{\text{rxn}} = 627.51 \cdot [\Sigma(G_{\text{tot}})_{\text{products}} - \Sigma(G_{\text{tot}})_{\text{reactants}}]_{\text{gas phase}} + \Sigma(G_{\text{solv}})_{\text{products}} - \Sigma(G_{\text{solv}})_{\text{reactants}} + \Delta nRT \ln(RT/P)$$

where Δn is the change in the number of moles in a balanced reaction equation when going from reactants to products. The standard state for all solutes is 1 M concentration and 55.5 M concentration for H_2O solvent.

3. Results and discussion

3.1. Reaction (eq 2) selectivity in methylammonium products **3** (**4**) and its rate law

^1H NMR spectroscopy was used to monitor concentrations of the reactant, $[\text{Pt}^{\text{IV}}\text{CH}_3\text{Cl}_5]^{2-}$, exhibiting the signal of its methyl ligand at 2.95 ppm, and the products, methylammonium cations **3** or methylpyridinium cations **4**, for which the integral intensity of their *N*-methyl group signals was measured. Formation of CH_3OH and CH_3Cl due to competitive reaction of $[\text{Pt}^{\text{IV}}\text{CH}_3\text{Cl}_5]^{2-}$ with water and chloride anions, respectively [6], was also monitored. The exact amount of MeCl could not be determined due to its distribution between solution and gas phases. In general, the observed rate constant for the disappearance of $[\text{Pt}^{\text{IV}}\text{CH}_3\text{Cl}_5]^{2-}$, $k_{\text{obs}}(\text{Pt}^{\text{IV}}\text{Me})$, is expected to be somewhat higher, as compared to the rate constant of formation of methylammonium cations, $k_{\text{obs}}(\text{MeN}^+)$, due to competitive reaction of $[\text{Pt}^{\text{IV}}\text{CH}_3\text{Cl}_5]^{2-}$ with water and chloride anions originating from KCl present in our samples of $\text{K}_2[\text{Pt}^{\text{IV}}\text{CH}_3\text{Cl}_5]$ as a major impurity in about 7: 1 KCl: $\text{K}_2\text{PtCl}_5\text{CH}_3$ molar ratio. In fact, in the case of *N,N*-dimethylaniline **1a** taken in 38-fold excess, both observed rates constants were almost identical within experimental error (Fig. 1a and b). This suggests realization of a selective methyl transfer to the amine in this case. Direct integration of MeOH and MeCl signals allows to find the upper estimate for the selectivity in **3a** of 99% whereas the yield of **3a** determined in the end of the reaction is its more accurate measure, 96% (Table 1 and S1).

For reactions involving other anilines **1b-1g** taken, typically, in 20–100 fold excess with respect to $\text{K}_2[\text{Pt}^{\text{IV}}\text{CH}_3\text{Cl}_5]$, the reaction selectivity in methylammonium products **3**, determined as yield of **3** in the end of reaction, ranged from 79% to 99% (Table 1 and S1). For 2,4,6-trimethylpyridine **2b** the best observed selectivity in **4b** was also high, 87%, whereas for the less reactive 2,6-dimethylpyridine **2a** and *N,N*-diisopropylaniline **1h** the reaction selectivity in the corresponding ammonium products was only 36% and 28%, respectively.

The reactions (eq 2) between $\text{K}_2[\text{Pt}^{\text{IV}}\text{CH}_3\text{Cl}_5]$ and amines **1** or **2** were run using anilines **1** or pyridines **2** taken in large excess, under pseudo-first order conditions. Typically, 0.40–8.4 mM solutions of $\text{K}_2[\text{Pt}^{\text{IV}}\text{CH}_3\text{Cl}_5]$ were used and the reactions were monitored for about 3 half-lives. In all of these cases the reactions followed pseudo-first order kinetics behavior (Fig. S1-S16). The reaction order in [amine] was analyzed using the parent compound of the anilines series, *N,N*-dimethylaniline **1a**. By varying concentration of the aniline **1a** in the range of 10–40 mM, a linear relationship was found between the observed pseudo-first order rate constant of the reaction, k_{obs} , and aniline concentration (Fig. 2). A similar dependence was also observed for 2,4,6-trimethylpyridine **2b** [22]. Hence, we conclude that the reaction (eq 2) is first order in the amine and first order in $\text{K}_2[\text{Pt}^{\text{IV}}\text{CH}_3\text{Cl}_5]$.

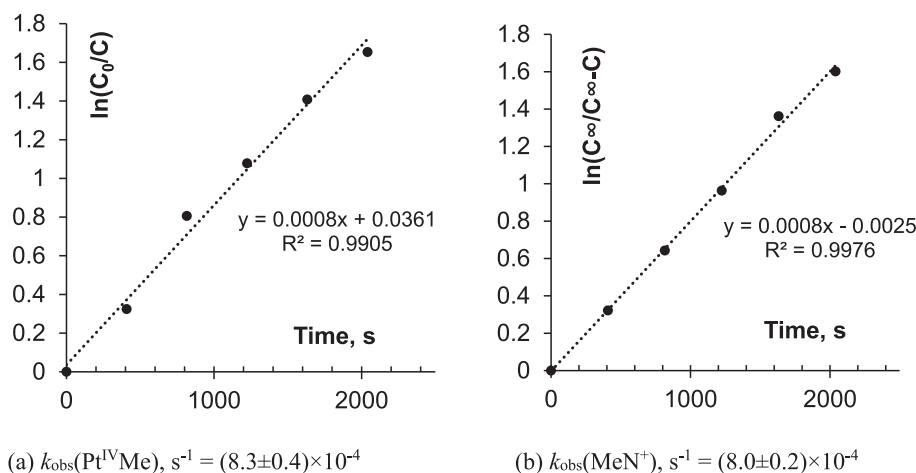


Fig. 1. Kinetic plots for reaction between $K_2[Pt^{IV}CH_3Cl_5]$ and N,N -dimethylaniline **1a** (eq 2) used in 38-fold excess, $[Pt^{IV}Me]_0 = 0.77$ mM, $[1a]_0 = 29.0$ mM: a) $\ln(C_0/C)$ plot produced by monitoring $[Pt^{IV}CH_3Cl_5]^{2-}$ signal at 2.95 ppm and b) $\ln(C_\infty/(C_\infty-C))$ plot produced by monitoring the NMe_2 group signal of **3a** at 3.68 ppm.

3.2. Reactivity of anilines **1**

The signal of the reactant $[Pt^{IV}CH_3Cl_5]^{2-}$ in 1H NMR spectra of $K_2[Pt^{IV}CH_3Cl_5]$ in 60% (vol.) aqueous acetone was observed at 2.95 ppm. The position of the signal did not change when the reagent was combined with anilines **1** or pyridines **2**. No new 1H NMR signals associated with $Pt^{IV}Me$ fragment were observed in the presence of the anilines **1a–1f**, **1h**, or pyridines **2**, so suggesting that no adducts of these amines and $Pt^{IV}CH_3$ formed in detectable amounts via amine for chloro ligand substitution. A very weak, ~5% of the intensity of the signal at 2.95 ppm, additional signal of $Pt^{IV}CH_3$ at 2.58 ppm was observed in reaction mixtures containing p - N,N,N',N' -tetramethylphenylenediamine and **1g** in 16: 1 ratio. This signal may result from a reaction of $[Pt^{IV}CH_3Cl_5]^{2-}$ with Pt-coordinating impurities present in our sample of **1g** (*vide infra*). In this case both $Pt^{IV}CH_3$ signals disappeared at the same rate. Overall, based on available observations, we can conclude that the steric and/or electronic properties of the amines **1a–1h** and **2** are sufficient to make ligand substitution at the Pt^{IV} center slow enough and/or thermodynamically unfavorable under the reaction conditions employed in our work. Hence, the second order rate constants k_2 found for **1a–1h** and **2a–2b** may be used as a correct measure of nucleophilicity of these amines with respect to electrophilic $[Pt^{IV}CH_3Cl_5]^{2-}$ or a derived aqua complex $[Pt^{IV}MeCl_4(H_2O)]^-$ (*vide infra*) [6] (eq (5)).

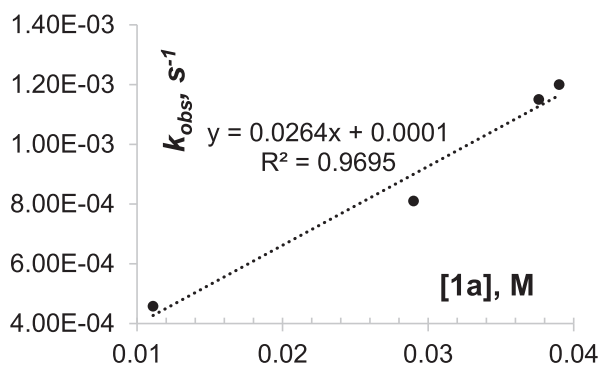


Fig. 2. Dependence of the observed pseudo-first order constant, k_{obs} , for reaction between $[Pt^{IV}CH_3Cl_5]^{2-}$ and N,N -dimethylaniline, **1a**, and the aniline concentration in 60% (vol.) aqueous acetone at 22 °C.



In the latter case, since ~7: 1 KCl: $K_2PtCl_5CH_3$ mixtures were used in all of our experiments, the KCl impurity may be expected to produce some inhibiting effect on the formation of the aqua complex $[Pt^{IV}MeCl_4(H_2O)]^-$ and the reaction (2) rates. At the same time, since the value of the equilibrium constant K_{eq} for the reaction (5) is close to 1 [6] and the solutions of $K_2[Pt^{IV}CH_3Cl_5]$ used in this work are very dilute, such effect should be negligible.

The second order rate constants for reaction of anilines **1** and pyridines **2** with $K_2[Pt^{IV}CH_3Cl_5]$ are summarized in Table 1. Their inspection shows that the reactivity of the studied pyridines **2a–2b** is inferior, as compared to N,N -dimethylaniline substrates **1a–1g**. The reactivities of these two groups of substrates are analyzed separately.

It is a common practice to use the pK_a values of nucleophiles of the same structural type as an approximate measure of their nucleophilicity [29]. Our analysis of the rate constants k_2 of N,N -dimethylanilines **1a–1g** shows that, indeed, there is a high-quality linear correlation between $\log(k_2)$ and pK_a values of the amines (Fig. 3, eq (6)):

$$\log(k_2) = 0.76pK_a - 5.55 \quad (6)$$

Table 1

Second order rate constants for methyl transfer from $[Pt^{IV}CH_3Cl_5]^{2-}$ to various amines (eq 2) measured in 60% (vol.) aqueous acetone solutions at 22 °C, yield of **3** or **4**^a in the end of reaction and the amines pK_a values.

	Amine	k_2 , $M^{-1} s^{-1b}$	Yield of 3 (4), % ^a	pK_a^c
1	1a (R = H)	$(2.6 \pm 0.3) \times 10^{-2}$	96	5.12 [23]
2	1b (R = <i>m</i> -Cl)	$(2.11 \pm 0.02) \times 10^{-3}$	79	3.83 [21]
3	1c (R = <i>p</i> -Cl)	$(4.71 \pm 0.02) \times 10^{-3}$	95	4.39 [21]
4	1d (R = <i>p</i> -Me)	$(5.15 \pm 0.07) \times 10^{-2}$	95	5.63 [24]
5	1e (R = <i>m</i> -Me)	$(2.85 \pm 0.02) \times 10^{-2}$	96	5.34 [24]
6	1f (R = <i>p</i> -MeO)	$(8.4 \pm 0.3) \times 10^{-2}$	98	5.85 [24]
7	1g (R = <i>p</i> -Me ₂ N)	0.174 ± 0.002^d	99	6.4 [25] ^d
8	1h	$(6.7 \pm 0.2) \times 10^{-4}$	28	7.4 [26]
9	2a	$(1.85 \pm 0.08) \times 10^{-5}$	36	6.73 [27]
10	2b	$(6.1 \pm 0.1) \times 10^{-4}$	87	7.48 [28]

^a Determined in the end of reaction as $100\% \times [3]$ (or $[4]$)/ $[K_2PtCl_5Me]_0$ with all concentrations derived from 1H NMR integration.

^b Average of two to four runs.

^c Aqueous solutions, 25 °C.

^d Statistically corrected for the number of NMe_2 groups.

The high quality of the correlation suggests that the electronic effects of the substituents present in the aniline core responsible for the change in the basicity of the amines are also responsible for the change in the amines nucleophilicity in methylation reaction (eq 2) with $[\text{Pt}^{\text{IV}}\text{CH}_3\text{Cl}_5]^{2-}$.

Considering the rate constants k_2 given in Table 1, it is also interesting to compare the electrophilicity of the $\text{K}_2[\text{Pt}^{\text{IV}}\text{CH}_3\text{Cl}_5]$ and that of some standard methylating agents used in organic chemistry. For *N,N*-dimethylaniline **1a** as a nucleophile in reaction (eq 2), its k_2 value, $0.026 \text{ M}^{-1} \text{ s}^{-1}$, is about an order of magnitude larger than second order rate constant $0.0021 \text{ M}^{-1} \text{ s}^{-1}$ reported for methylation of this amine with dimethylsulfate, $(\text{CH}_3)_2\text{SO}_4$, in sulfolane as a solvent at 30°C [30]. Similarly, a comparison of reactivity of *p*-*N,N,N',N'*-tetramethylphenyldiamine **1g** toward $\text{K}_2[\text{Pt}^{\text{IV}}\text{CH}_3\text{Cl}_5]$ (eq 2) and dimethylsulfate (sulfolane, 30°C) shows that the second order rate constant for the former reaction, $0.174 \text{ M}^{-1} \text{ s}^{-1}$, is about 3 times greater than the rate constant for the second process, $0.059 \text{ M}^{-1} \text{ s}^{-1}$ [30]. Hence, $\text{K}_2[\text{Pt}^{\text{IV}}\text{CH}_3\text{Cl}_5]$ is approximately as electrophilic as $(\text{CH}_3)_2\text{SO}_4$.

Among all the anilines **1** studied in reaction (eq 2), the *N,N*-diisopropylaniline **1h** is the least reactive with its $\log(k_2)$ value deviating by 3.3 orders of magnitude from the linear correlation (eq (6)) established for **1a–1g**. The most likely origin of this deviation/diminished nucleophilicity is the steric bulk of two isopropyl groups at the nucleophilic nitrogen center that interfere with its approach to the $\text{Pt}^{\text{IV}}\text{CH}_3$ electrophile.

3.3. Reaction of $\text{K}_2[\text{Pt}^{\text{IV}}\text{CH}_3\text{Cl}_5]$ with the aniline **1g**

The aniline **1g** is the most reactive, most nucleophilic and most reducing [25] among the anilines studied in this work. As compared to other anilines **1a–1f**, this compound is readily oxidized in aqueous solutions when exposed to air, so that its solutions may contain some small amounts of derived impurities. Because of this sensitivity to O_2 , all the work with this amine was carried out under

argon atmosphere. Notably, no signals of the compound could be observed in its ^1H NMR spectra in 60% (vol.) aqueous acetone solutions, although a clean ^1H NMR spectrum of **1h** could be produced in CDCl_3 . Upon combination of **1g** and $\text{K}_2[\text{Pt}^{\text{IV}}\text{CH}_3\text{Cl}_5]$ in aqueous acetone, the solution color immediately turned light blue and, as the methyl transfer reaction (eq 2) progressed, four sharp signals attributed to the reaction product **3g** appeared and continued to grow, two singlets at 3.57 ppm (9H, Me_3N^+) and 2.89 ppm (6H, Me_2N), and two AX doublets of the aromatic protons at 6.77 and 7.63 ppm. The blue color observed in our reaction mixtures is likely associated with the formation of the amine cation radical reported earlier for this compound and produced by catalytic oxidation of aqueous **1g** with H_2O_2 [25]. In spite of these observations that may suggest a possible change in the mechanism of the methyl transfer from $[\text{Pt}^{\text{IV}}\text{CH}_3\text{Cl}_5]^{2-}$ to the amine, the reaction (eq 2) rate constant does not deviate from the trend (eq (6)) established for all *N,N*-dimethyl anilines studied here. Hence, the dominant reaction path for this amine is likely to involve an $\text{S}_{\text{N}}2$ mechanism.

3.4. Reactivity of pyridines **2a–2b**

As it was mentioned earlier and is shown in Fig. 3, pyridines **2a–2b** are the least reactive among the nucleophiles explored here. Their low nucleophilicity may be attributed, in particular, to the steric bulk created by two methyl groups in the positions 2 and 6 of the pyridine ring. In turn, the 33-fold increase in nucleophilicity of **2b**, in response to the electronic effect of the methyl group *para*-to the pyridine nitrogen, as compared to 2,6-dimethylpyridine **2a**, is much greater than the effect of the *para*-methyl substituent in *N,N*-dimethyl-*para*-toluidine **1d**, as compared to the parent *N,N*-dimethylaniline **1a**. In the latter case, an about 2-fold nucleophilicity increase is observed for **1d**, as compared to **1a**. A fewer number of bonds separating nucleophilic nitrogen atom and the methyl substituent in **2b** vs. **1d** may, in part, be responsible for the difference.

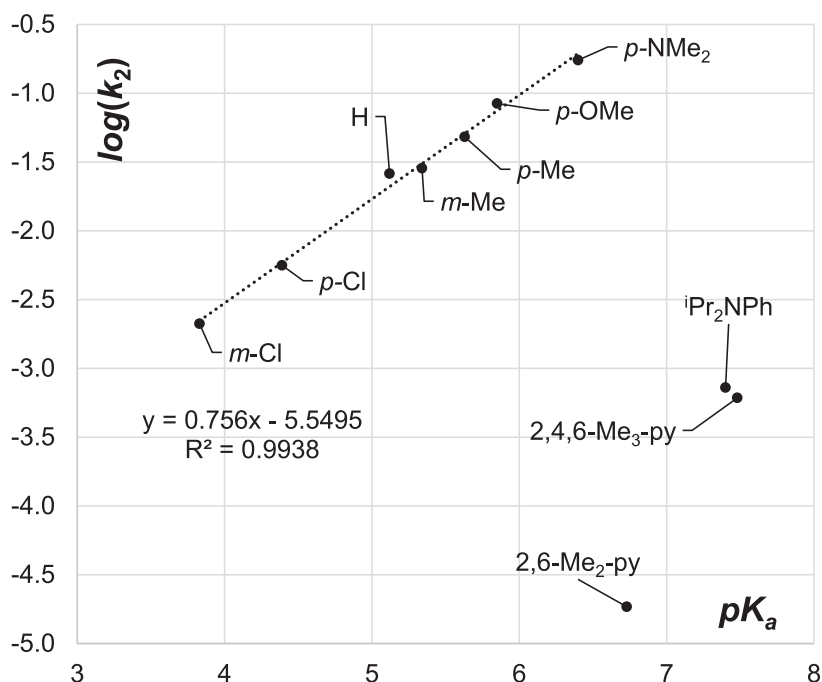
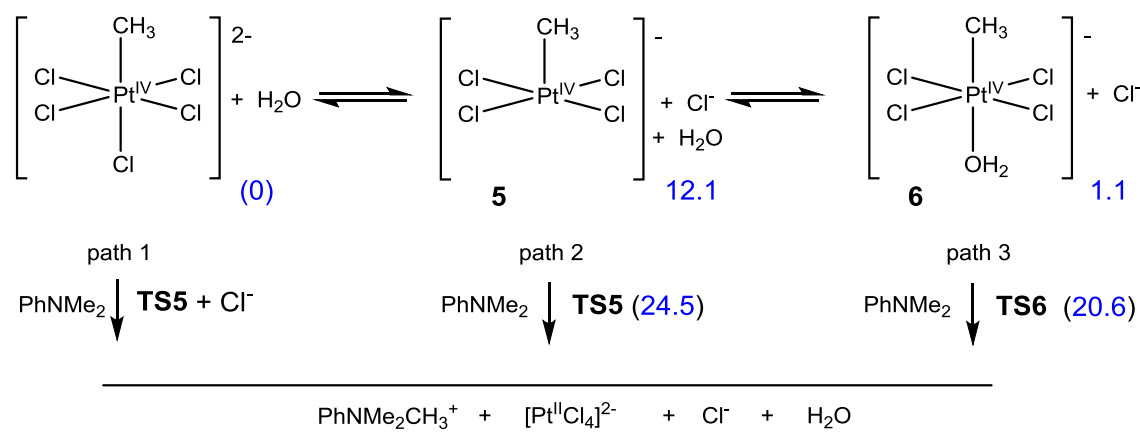


Fig. 3. The reactivity of amines **1, 2**, $\log(k_2)$, with respect to $[\text{Pt}^{\text{IV}}\text{CH}_3\text{Cl}_5]^{2-}$ (eq 2) in 60% (vol.) aqueous acetone at 22°C as a function of the amines pK_a .



Scheme 2. Methyl transfer from various Pt^{IV}CH₃ species to PhNMe₂, **1a**, in aqueous media. Numbers in blue font are the DFT-calculated Gibbs energies for the corresponding aqueous solutions under standard conditions (1 M solutions, 25 °C).

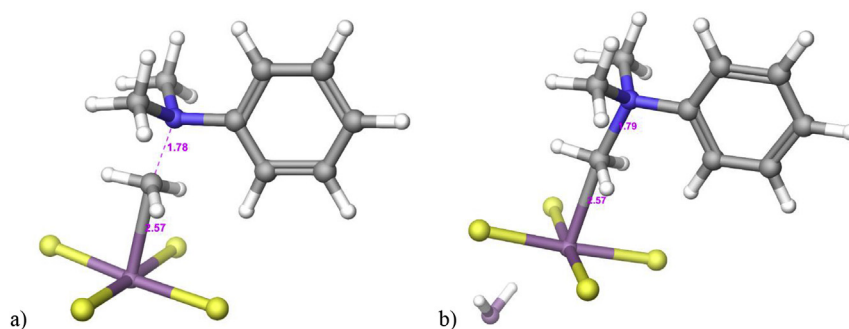


Fig. 4. Structures of the S_N2-type reaction transition states in Scheme 2: a) the **TS5** located for the pathway 2, b) the **TS6** found for the pathway 3.

3.5. Computational (DFT) analysis of reaction between [Pt^{IV}CH₃Cl₅]²⁻ and anilines **1**

Previously [6] two possible methyl transfer pathways were considered for the systems comprised of aqueous [Pt^{IV}CH₃Cl₅]²⁻ and water or chloride anion as nucleophiles, one involving 5-coordinate Pt^{IV} transient species [Pt^{IV}CH₃Cl₄]⁻, **5**, (Scheme 2) and another involving the derived aqua complex [Pt^{IV}CH₃Cl₄(H₂O)]⁻, **6**. Two corresponding pathways shown in Scheme 2 for the case of *N,N*-dimethylaniline **1a** as a nucleophile are pathways 2 and 3, respectively. For the completeness of the analysis, one more reaction path, pathway 1, is also added to Scheme 2 that includes the starting 6-coordinate complex [Pt^{IV}CH₃Cl₅]²⁻.

The three pathways in Scheme 2 have been analyzed computationally (DFT) in this work using modeling of pure water as a solvent. The 5-coordinate transient **5** was found to be 12.1 kcal/mol higher in energy than [Pt^{IV}CH₃Cl₅]²⁻, and the corresponding reaction pathway 2 leads to a relatively low energy ‘classic’ S_N2-type reaction transition state **TS5** (Fig. 4a) with the overall Gibbs energy of 24.5 kcal/mol. For the 6-coordinate complex [Pt^{IV}CH₃Cl₅]²⁻ (pathway 1), no individual transition state could be found. In this case, our transition state search converges to a combination of a ‘free’ non-coordinated chloride anion and the **TS5**. Hence, the reaction path 1 does not include a mechanism that would be kinetically more competitive, as compared to pathway 2. Finally, the 6-coordinate transient aqua complex [Pt^{IV}CH₃Cl₄(H₂O)]⁻, **6**, is 1.1 kcal/mol higher in energy than [Pt^{IV}CH₃Cl₅]²⁻, a good match to

an experimental estimate of ~0 kcal/mol Gibbs energy change for the aqua-for-chloro ligand substitution in [Pt^{IV}CH₃Cl₅]²⁻ [6]. Remarkably, the reaction pathway 3 leads to the transition state **TS6** (Fig. 4b) which, similar to pathway 1, corresponds to a loss of the ligand *trans*-to the methyl happening well before the C–Pt/C–N bond breaking/making event. But, in contrast to pathway 1, in the transition state **TS6** the former H₂O ligand remains hydrogen-bonded to two adjacent chloro ligands of the leaving group [Pt^{III}Cl₄]²⁻ with the two shortest Cl...HO distances of 2.48 Å each. Comparing other key parameters of the transition states **TS5** and **TS6**, one can conclude that they are very close, with the Pt–C and (Pt)C–N distances being essentially the same in both species. Hence, **TS6** may be viewed as a hydrogen bond - stabilized version of the **TS5** where an explicit water molecule helps to better account for the transition state interaction with the solvent. The calculated Gibbs energy for **TS6** is 20.6 kcal/mol, a good match to the experimental value of 19.4 kcal/mol. Hence, we can conclude that: i) the methyl transfer from [Pt^{IV}CH₃Cl₅]²⁻ to the aniline **1a** proceeds via the 5-coordinate Pt^{IV}CH₃ transient **5** and ii) a proper account for the solvation/hydrogen bonding between reacting solutes and water solvent is important for achieving better match of experimental and calculated reaction activation energies.

4. Conclusions

The reaction of K₂[Pt^{IV}CH₃Cl₅], *N,N*-dimethylamines and 2,6-disubstituted pyridines studied here (eq 2) follows a ‘simple’

second order reaction kinetics with first order in both the amines and $K_2[Pt^{IV}CH_3Cl_5]$. Remarkably, $K_2[Pt^{IV}CH_3Cl_5]$ complex is about as reactive as a methyl transfer agent as a typical organic methylating agent, dimethylsulfate. In turn, among the substrates studied, the *N,N*-dimethylanilines **1a–1g** react at about 100–1000 times faster rates than 2,6-dimethylpyridines **2a** and **2b** or *N,N*-diisopropylaniline **2h**, thanks, most likely, to the greater steric bulk of the alkyl substituents near the nucleophilic nitrogen atom in the latter three substrates. A high quality linear free energy relationship was found between logarithm of second order rate constants for the methyl transfer reaction (eq 2) and pK_a of the dimethylanilines **1a–1g**. A computational (DFT) analysis of the reaction (eq 2) is consistent with the realization of S_N2 mechanism where 5-coordinate Pt^{IV} transient electrophile $[Pt^{IV}CH_3Cl_4]^-$ is attacked by the amines.

Acknowledgements

This work was supported by the National Science Foundation, USA (CHE-1464772, CHE-1800089).

Appendix A. Supplementary data

Supplementary data to this article can be found online at <https://doi.org/10.1016/j.jorganchem.2018.10.020>.

References

- [1] N.F. Gol'dshleger, V.V. Es'kova, A.E. Shilov, A.A. Shteinman, Reactions of alkanes in solutions of chloride complexes of platinum, *Zh. Fiz. Khim.* 46 (1972) 1353–1354.
- [2] a) A.E. Shilov, G.B. Shulpin, *Activation and Catalytic Reactions of Saturated Hydrocarbons in the Presence of Metal Complexes*, Kluwer, Boston, 2000; b) J.A. Labinger, J.E. Bercaw, Mechanistic studies of the Shilov system: a retrospective, *J. Organomet. Chem.* 793 (2015) 47–53.
- [3] Yu.V. Geletii, A.E. Shilov, Catalytic oxidation of alkanes by molecular oxygen - oxidation of methane in the presence of platinum salts and heteropoly acids, *Kinet. Catal.* 24 (1983) 413–416.
- [4] I. Bar-Nahum, A.M. Khenkin, R. Neumann, Mild, aqueous, aerobic, catalytic oxidation of methane to methanol and acetaldehyde catalyzed by a supported bipyrimidinylplatinum-polyoxometalate hybrid compound, *J. Am. Chem. Soc.* 126 (2004) 10236–10237.
- [5] J.E. Kreutz, A. Shukhaev, W. Du, S. Druskin, O. Daugulis, R.F. Ismagilov, Evolution of catalysts directed by genetic algorithms in a plug-based microfluidic device tested with oxidation of methane by oxygen, *J. Am. Chem. Soc.* 132 (2010) 3128–3132.
- [6] a) G.A. Luinstra, L. Wang, S.S. Stahl, J.A. Labinger, J.E. Bercaw, C-H Activation by aqueous platinum complexes: a mechanistic study, *J. Organomet. Chem.* 504 (1995) 75–91; b) E.S. Rudakov, G.B. Shul'pin, Stable organoplatinum complexes as intermediates and models in hydrocarbon functionalization, *J. Organomet. Chem.* 793 (2015) 4–16.
- [7] G.A. Luinstra, J.A. Labinger, J.E. Bercaw, Mechanism and stereochemistry for nucleophilic attack at carbon of platinum(IV) alkyls: model reactions for hydrocarbon oxidation with aqueous platinum chlorides, *J. Am. Chem. Soc.* 115 (1993) 3004–3005.
- [8] T.E. Stevens, K.A. Smoll, K.I. Goldberg, Direct formation of carbon(sp³)-heteroatom bonds from Rh^{III} to produce methyl iodide, thioethers, and alkylamines, *J. Am. Chem. Soc.* 139 (2017) 7725–7728.
- [9] M. Kirchgessner, K. Sreenath, K.R. Gopidas, Understanding reactivity patterns of the dialkylaniline radical cation, *J. Org. Chem.* 71 (2006) 9849–9852, <https://doi.org/10.1021/jo061809i>.
- [10] R.S. Lewis, M.F. Wisthoff, J. Grissmerson, W.J. Chain, Metal-free functionalization of *N,N*-dialkylanilines via temporary oxidation to *N,N*-dialkylaniline *N*-oxides and group transfer, *Org. Lett.* 16 (2014) 3832–3835, <https://doi.org/10.1021/ol501813s>.
- [11] J.T. Reeves, D.R. Fandrick, Z. Tan, J.J. Song, H. Lee, N.K. Yee, C.H. Senanayake, Room temperature palladium-catalyzed cross coupling of aryl-trimethylammonium triflates with aryl grignard reagents, *Org. Lett.* 12 (2010) 4388–4391, <https://doi.org/10.1021/ol1018739>.
- [12] G.F. Silbestri, M.T. Lockhart, A.B. Chopa, Two-step synthesis of di- and tris-tannylarenes from anilines via an $S_{RN}1$ mechanism, *Org. Chem. Argentina* 7 (2011) 210–220, <https://doi.org/10.3998/ark.5550190.0012.718>.
- [13] D.Y. Wang, Z.K. Wang, C. Wang, A. Zhang, M. Uchiyama, From anilines to aryl ethers: a facile, efficient, and versatile synthetic method employing mild conditions, *Angew. Chem. Int. Ed.* 57 (2018) 3641–3645, <https://doi.org/10.1002/anie.201712618>.
- [14] H. Zhang, S. Hagihara, K. Itami, Making dimethylamino a transformable directing group by nickel-catalyzed C–N borylation, *Chem. Eur. J.* 21 (2015) 16796–16800, <https://doi.org/10.1002/chem.201503596>.
- [15] Z. Feng, J.L. Tao, Z.X. Wang, Palladium-catalyzed C–H arylation of (benzo)oxazoles or (benzo)thiazoles with aryltrimethylammonium triflates, *Org. Lett.* 17 (2015) 4926–4929.
- [16] J. Hu, H. Sun, W. Cai, X. Pu, Y. Zhang, Z. Shi, Nickel-catalyzed borylation of aryl- and benzyltrimethylammonium salts via C–N bond cleavage, *J. Org. Chem.* 81 (2016) 14–24, <https://doi.org/10.1021/acs.joc.5b02557>.
- [17] N.V. Ignat'ev, P. Barthen, A. Kucheryna, H. Willner, P. Sartori, A convenient synthesis of triflate anion ionic liquids and their properties, *Molecules* 17 (2012) 5319–5338, <https://doi.org/10.3390/molecules17055319>.
- [18] R.G. Parr, W. Yang, *Density-functional Theory of Atoms and Molecules*, Oxford University Press, Oxford, 1989.
- [19] J.P. Perdew, K. Burke, M. Ernzerhof, Generalized gradient approximation made simple, *Phys. Rev. Lett.* 77 (1996) 3865–3868.
- [20] Jaguar, Version 8.4, Schrödinger, LLC, New York, NY, 2014.
- [21] W.M. Haynes (Ed.), *CRC Handbook of Chemistry and Physics*, 97th Edition, CRC Press, New York, 2017.
- [22] See Supporting Information for details.
- [23] J.L. Jensen, A.T. Thibeault, The basicity of enones. Substituent effects and the correlation of protonation with HA, *J. Org. Chem.* 42 (1977) 2168–2170.
- [24] M.M. Fickling, A. Fischer, B.R. Mann, J. Parker, J. Vaughan, Hammett substituent constants for electron-withdrawing substituents: dissociation of phenols, anilinium ions and dimethylanilinium ions, *J. Am. Chem. Soc.* 81 (1959) 4226–4230.
- [25] K. Krikstopaitis, J. Kulyš, A.H. Pedersen, P. Schneider, *N*-substituted *P*-phenylenediamines as peroxidase and laccase substrates, *Acta Chem. Scand.* 52 (1998) 469–474.
- [26] M. Sobkowski, J. Stawinski, A. Kraszewski, Stereochemistry of internucleotide bond formation by the H-phosphonate method. 5. The role of bronsted and H-bonding base catalysis in ribonucleoside H-phosphonate condensation-chemical and stereochemical consequences, *Nucleos. Nucleot. Nucleic Acids* 29 (2010) 628–645.
- [27] H.C. Brown, X.R. Mihm, Steric effects in displacement reactions. III. The base strengths of pyridine, 2,6-lutidine and the monoalkylpyridines, *J. Am. Chem. Soc.* 77 (1955) 1723–1726.
- [28] K. Clarke, K. Rothwell, A kinetic study of the effect of substituents on the rate of formation of alkylpyridinium halides in nitromethane solution, *J. Chem. Soc.* (1960) 1885–1895, 377.
- [29] E.V. Anslyn, D.A. Dougherty, *Modern Physical Organic Chemistry*, University Science, Sausalito, CA, 2006.
- [30] E.S. Lewis, S. Kukes, C.D. Slater, Reactivity in methyl transfer reactions. 4. Powerful methylating agents with neutral nucleophiles, *J. Am. Chem. Soc.* 102 (1980) 303–306.